Pergamon

Bioorganic & Medicinal Chemistry, Vol. 3, No. 9, pp. 1273–1280, 1995

0968-0896/95 $9.50 + .00

0968-0896(95)00122-0

Solution Structure of Endothelin B Receptor Selective Antagonist RES-701-1 Determined by ^{1}H NMR Spectroscopy

Ritsuko Katahira, Kenji Shibata, Motoo Yamasaki, Yuzuru Matsuda and Mayumi Yoshida*

Tokyo Research Laboratories, Kyowa Hakko Kogyo Co. Ltd, 3-6-6, Asahimachi, Machida-shi, Tokyo 194, Japan

Abstract—The three-dimensional structure of the endothelin B receptor (ET_B) selective antagonist RES-701-1 has been determined by ^{1}H NMR in deuterated dimethyl sulphoxide. RES-701-1 consists of 16 amino acid residues with a novel internal linkage between the β-carboxyl group of Asp9 and the α-amino group of Gly1. The structural calculations were carried out with the combined use of distance geometry and simulated annealing. The result indicates that RES-701-1 adopts an extraordinary folding; the 'tail' (Trp10–Trp16) passes through the 'ring' region (Gly1–Asp9). Several critical NOEs directly support this extraordinary folding. The folding of RES-701-1 turned out to be the same as that Frèchet *et al.* calculated for RP 71955 which possesses the same internal linkage as RES-701-1. The obtained structure suggested that the region consisting of Thr6, Ala7, Tyr14 and Tyr15 and/or, the region consisting of Asn2, Tyr14 and Tyr15 are involved in a binding with ET_B.

Introduction

Endothelin-1 (ET-1), first isolated from endothelial cells, is a 21 amino acid peptide with two disulfide bonds. It exhibits the most potent and long lasting activity of any vasoconstrictor known.[1] Two isoforms (ET-2, ET-3) have been identified so far.[2] These three peptides mediate many biological responses in cardiovascular and non-cardiovascular tissue through binding to two different types of receptors, ET_A and ET_B. The amino acid sequences of ET-1, -2 and -3 are listed in Figure 1. ET_A exhibits the affinity rank order: ET-1 ≥ ET-2 > ET-3[3–5], and ET_B possesses similar affinities for all three endothelins.[6–8] ET-3 is a relatively selective ET_B agonist. Since ET-receptor antagonists may possess therapeutic efficiency in cardiovascular disease, renal disease and asthma,[9] extensive efforts to understand their structure–activity relationships have been conducted in recent years. In order to obtain structural information, the solution structures of ET receptor ligands have been studied by ^{1}H NMR.[10–17] The consensus structure between ET-1 and ET-3 has been shown to be helical between the residues Lys9 and Cys15. The structure of the C-terminal hexapeptide remains obscure due to the different solvent systems used in the experiments. The C-terminal region of ET-3 was proposed to fold back towards the helical region, resulting in the formation of the hydrophobic core that was considered to be indispensable for activity.[10]

In addition to the study on ET-receptor agonists, it is essential to find specific ET-receptor antagonists to elucidate the physiological and pathophysiological significance of ET. We have isolated a novel ET_B selective antagonist RES-701-1 (IC_{50} = 10 nM).[18] The amino acid sequence is indicated in Figure 1. The primary structure of RES-701-1 was determined by the sequencing of peptide fragments obtained by limited chemical hydrolysis, and FABMS spectroscopy.[19] This antagonist possesses a novel structure, i.e., an internal linkage between the β-carboxyl group of Asp9 and the α-amino group of Gly1. Thus it is divided into two regions, i.e., the 'ring' (Gly1–Asp9) and the 'tail' (Trp10–Trp16).

There are many publications on the three-dimensional (3-D) structures of ET_A selective antagonists such as BQ-123 and BE-18257B.[20–23] However, there have been no reports on that of an ET_B selective antagonist. Here we show the 3-D structure of the ET_B selective antagonist, RES-701-1, based on ^{1}H NMR, combined calculations of distance geometry (DG) and simulated annealing (SA), and NOESY back calculations using a full-relaxation matrix. The resulting structure is compared with the solution structure of RP 71955 determined by Frèchet *et al.*,[24] which possesses the same internal linkage as RES-701-1 (Fig. 1). The structure–activity relationship of RES-701-1 is discussed on the basis of the receptor binding affinities of RES-701-1 derivatives, the solution structure of ET-3 reported by Mills *et al.*[10] and the nonselective antagonist, SB209670[25] (Fig. 1). The structures of ET_B selective antagonists are expected to broaden our understanding of the difference in ligand-binding affinity between ET_B and ET_A.

Results

Sequential assignments and secondary structure elements

Assignments of the proton resonances were performed by the sequence specific assignment strategy of Wüthrich.[26] The proton chemical shifts of RES-701-1 are listed in Table 1. The type and relative intensities

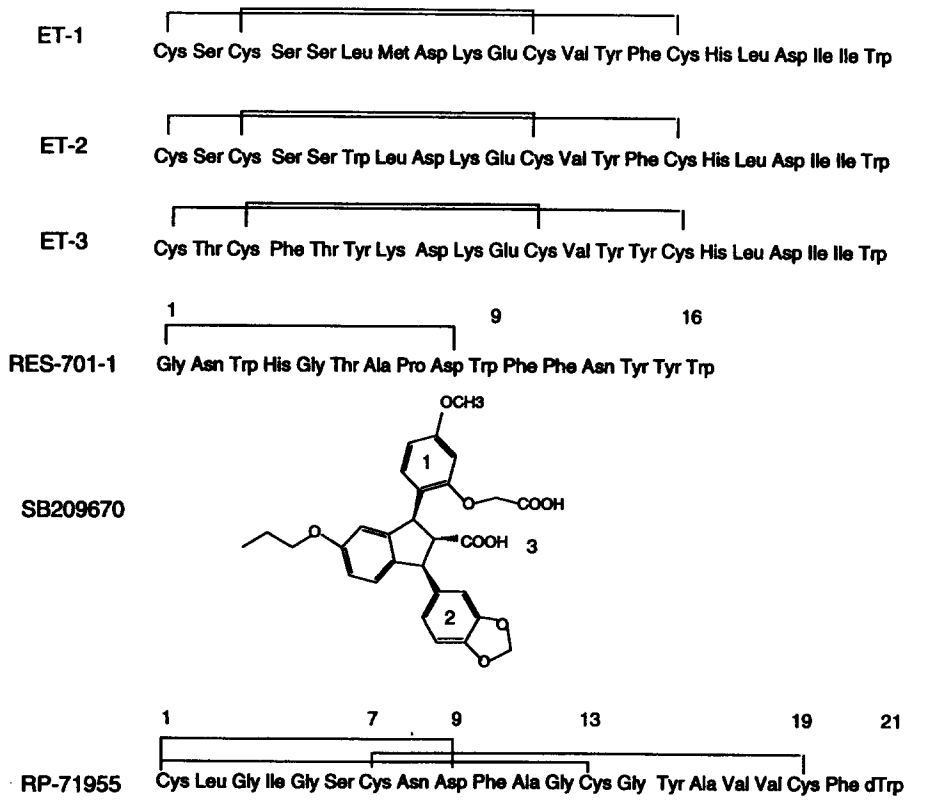

Figure 1. Amino acid sequence of ET-1, ET-2, ET-3, RES-701-1, SB209670 and RP 71955. For the labeling of SB209670, see Discussion.

of the sequential and longer NOEs are summarized in Figure 2, these can yield clues to identify the secondary structures. A strong $d_{\alpha\alpha(i,j)}$ NOE between the CαH of Pro8 and Asn13, a strong $d_{\alpha N(i,j)}$ NOE between the CαH of Asn13 and the NH of Asp9, and a weak $d_{\alpha N(i,j)}$ NOE between the CαH of Pro8 and the NH of Tyr14 were observed (Fig. 2). These NOEs reveal the presence of an antiparallel β-sheet structure formed between the segments Ala7 to Asp9 and Phe12 to Tyr14. Observation of a weak $d_{\alpha N(i,i+2)}$ NOE between the residues Gly5 and Ala7 indicates the presence of a turn like structure. The presence of a strong NOE between the CαH of Ala7 and the CδH of Pro8 indicates the exclusive adoption of a *trans* peptide bond. The strong sequential $d_{\alpha N}$ NOEs for the Asn13–Trp16 region suggest an extended structure. In addition, several NOEs indicating an interaction between the 'tail' and 'ring' regions were observed (Fig. 2). Especially the Asn13CβH–Gly5NH NOE, the Asn13CβH–Gly5CαHs NOEs and the Asn13NH_2–His4CαH NOE suggest that the sidechain of Asn13 is close to the backbone atoms of the His4–Gly5 segment of the 'ring'.

Table 1. ^{1}H Chemical shift Table of RES-701-1 in DMSO at 30 °C*

residue	NH	CαH	CβH	others
G1	8.54	4.25,3.50		
N2	9.10	4.92	Hβ3 2.46,Hβ2 3.20	NH_2 7.51,7.20
W3	8.06	4.36	2.91	H2 6.94,H4 7.42,H5 6.83,H6 7.02,H7 7.30, NH 10.78
H4	7.64	4.82	Hβ3 2.76,Hβ2 3.00	H2 9.07,H4 6.89
G5	7.97	4.40,3.60		
T6	7.92	4.33	4.41	γMe 1.10
A7	7.86	4.76	1.22	
P8		4.96	2.00	γH 1.88,1.96, δH 3.68
D9	7.64	4.53	2.66, 3.08	
W10	7.80	4.00	Hβ3 3.06, Hβ2 2.84	H2 6.92,H4 7.42,H5 6.96,H6 7.02, H7 7.30, NH 10.73
F11	7.22	4.38	2.53,2.62	H2,6 6.95,H3,5 7.16,H4 7.24
F12	8.54	4.25	Hβ3 3.22,Hβ2 2.80	H2,6 6.95,H3,5 7.16 H4 7.28
N13	8.02	5.48	Hβ3 1.98,Hβ2 2.25	NH_2 6.76,6.53
Y14	8.49	4.83	2.66	H2,6 6.90, H3,5 6.60
Y15	8.43	4.51	2.84	H2,6 6.88, H3,5 6.53
W16	7.57	4.43	Hβ3 2.84,Hβ2 3.06	H2 7.23,H4 7.47,H5 6.96,H6 7.02,H7 7.33, NH 10.48

*Chemical shifts are referenced internally to the methyl resonance of DMSO-d_6 at 2.5 ppm.

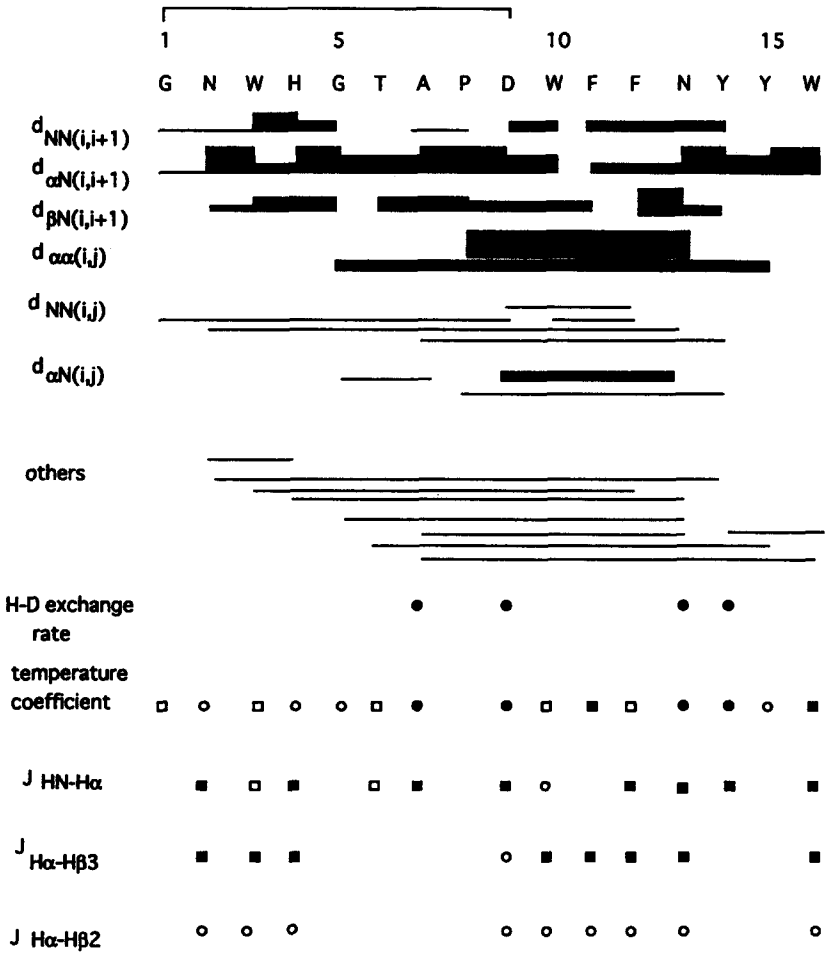

Figure 2. NOE connectivities and coupling constants of RES-701-1. The thickness of bars indicates the intensity of NOE cross peaks. The CδH proton was substituted for the NH proton for Pro8. For H–D exchange rate, closed circle indicates that the H–D exchange rate was very slow (see text). For temperature coefficients, open circle indicates that $5 \leq \Delta\delta/\Delta T$, open square, that $3 \leq \Delta\delta/\Delta T < 5$, closed square, $1 \leq \Delta\delta/\Delta T < 3$ ppb K^{-1}, closed circle, $\Delta\delta/\Delta T < 1$ ppb K^{-1}. For coupling constants, a closed square indicates that $J \geq 9$ Hz, an open square, that $5 \leq J < 9$ Hz, an open circle, that $J < 5$ Hz.

Determination of the three dimensional structure

After the DADAS calculations, 50 structures with best-satisfied NMR restraints were used for further SA refinements. Figure 3 shows the backbone atoms of 46 refined structures of RES-701-1. This figure shows that RES-701-1 adopts an extraordinary folding; the 'tail' region passes through the 'ring' region. Table 2 shows the structural statistics and the root mean square deviation (rmsd) values of RES-701-1. The energies due to the constraints (E noe and E cdih in Table 2) were low in comparison with the total energy. For the 46 accepted structures among the 50 calculated ones, the distance constraint violations were less than 0.2 Å and angle constraint violations were less than 5°. The root mean square (rms) differences for angle deviations from the ideal were less than 2° and rms differences for bond deviations from the ideal were less than 0.01 Å. The average rmsd per residue for 46 accepted structures is shown in Figure 4. The backbone atoms of all residues except Trp16 are well defined. The sidechain orientations of Trp3, Trp10, Phe11, Tyr15 and Trp16 were not well defined. This is probably due to the fact that the aromatic ring protons of these residues, except Trp16, did not give any inter-residue NOE. A systematic analysis of the obtained structures was undertaken using the ϕ and ψ angle by X-PLOR. Calculated structures

Table 2. Structural statistics of RES-701-1

X-PLOR potential energies	
E total (kcal mol^{-1})	28.51 ± 0.56
E bond	1.28 ± 0.04
E angle	25.19 ± 0.29
E improper	1.62 ± 0.07
E vdw	0.29 ± 0.18
E noe	0.06 ± 0.08
E cdih	0.01 ± 0.02
Rmsd from idealized geometry used within X-PLOR	
bond (Å)	0.00 ± 0.00
angle (degree)	0.59 ± 0.00
improper (degree)	0.23 ± 0.00
Rmsd from experimental restraints	
noe (Å)	0.00 ± 0.00
cdih (degree)	0.05 ± 0.06
Rmsd (Å)	
back bone (1–15)	0.51 ± 0.31
heavy atoms (1–15)	1.51 ± 0.51

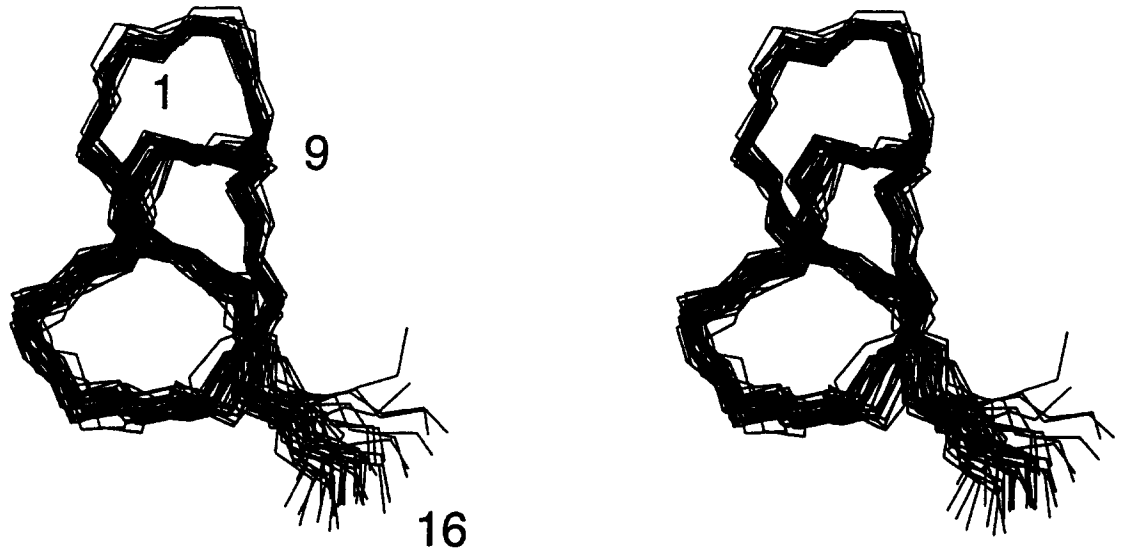

Figure 3. Stereoview of backbone atoms (N, Cα, C) and the linkage carbons (Cβ and Cγ of Asp9) of a family of 46 structures of RES-701-1. The structures were each superimposed for minimum pairwise rmsd values of the back bone atoms.

which satisfied NMR constraints possessed no ϕ and ψ angles in the forbidden region (data not shown).

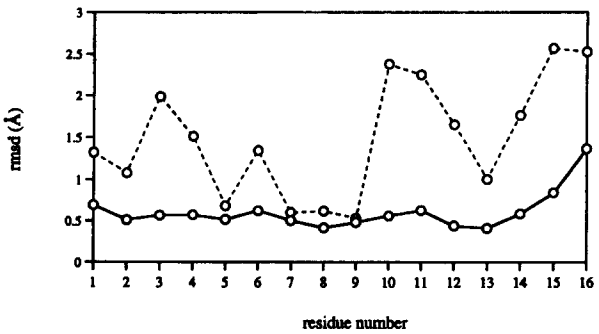

Figure 4. Average rmsd of the structures refined by X-PLOR. Solid line indicated backbone atoms and dashed line, heavy atoms.

The average structure of 46 SA structures was directly refined to the NOE intensities by monitoring the R-factor. For the R-factor, values of 0.123 and 0.103 were obtained before and after the refinement, respectively. The empirical terms of X-PLOR energy hardly changed after the refinement. A value of 3 ns was found to give the best consistency between the calculated and observed NOE intensities. Figure 5 shows the ribbon representation of backbone atoms with the heavy atoms of the sidechains of the refined structure.

Discussion

Structural consideration and comparison with the structure of RP 71955

We have determined the three dimensional structure of the ET_B selective antagonist, RES-701-1. The resulting

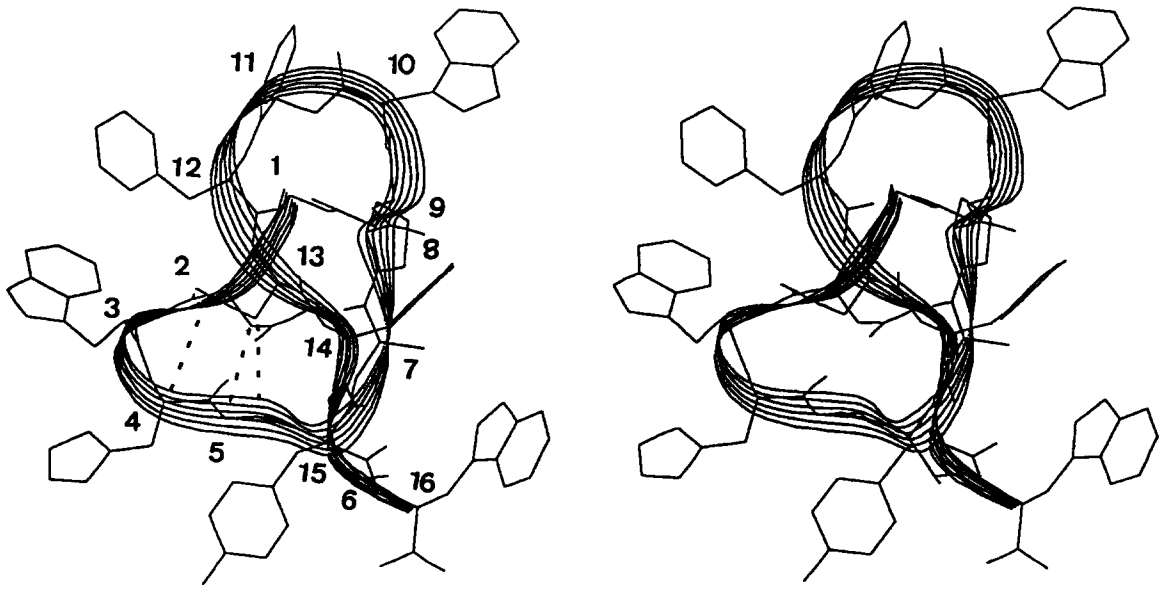

Figure 5. Ribbon representation of RES-701-1. Shown is the structure obtained after the direct refinement to NOE intensities. For the dotted lines, see text.

structure indicated that RES-701-1 adopts a novel and extraordinary structure, i.e., the 'tail' passes through the 'ring' region. As shown in Figure 5, the Phe12–Asn13 segment of the 'tail' lies above the Gly1–Trp3 of the 'ring', and the Tyr14–Tyr15 segment of the 'tail' is found below the Gly5–Ala7 of the 'ring'. There are two possible cases concerning the relative position of the Phe12–Asn13 segment to the Gly1–Trp3 segment. One is that the Phe12–Asn13 segment is above the Gly1–Trp3, and the other is below. Similarly there are two possible cases concerning the relative position of the Tyr14–Tyr15 segment to the Gly5–Ala7 segment. Here we consider why the relative positions between the above segments are defined, as shown in Figure 5.

The Ala7–Asp9 and Phe12–Tyr14 segments form a β-sheet structure with the Pro8 CαH and the Asn13 CαH located 'face-to-face', as supported by a strong NOE between them. In Figure 5, the proline ring of Pro8 is located above the backbone ribbon of the Ala7–Asp9 segment. In β-sheet structures, the sidechains of two consecutive residues stick out in opposite directions with respect to the backbone ribbon. Thus the sidechain of Asp9 which is the next residue to Pro8 is below the backbone ribbon of the Ala7–Asp9 segment. Since the sidechain of Asp9 makes linkage with Gly1, the Gly1–Trp3 segment could not be above the backbone ribbon of the antiparallel β-sheet segments in Figure 5. Thus the Phe12–Asn13 segment must be above the Gly1–Trp3. The relative position of the Phe12–Asn13 segment to the Gly1–Trp3 segment is defined in this way.

Several NOEs were observed between the sidechains of Asn13 and the backbone atoms of the His4–Gly5 segment of the 'ring' (Fig. 5, dotted lines). This indicated that the sidechain of Asn13 is close to the backbone of the His4–Gly5 segment of the 'ring'. As discussed above, the Phe12–Asn13 segment lies above the Gly1–Trp3. If one tries to put the sidechain of Asn13 close to the backbone protons of the His4–Gly5 segment under these circumstances, the Tyr14–Tyr15 segment must be located below the Gly5–Ala7 segment to avoid steric hindrance from the sidechain of Tyr14. It should be noted that the sidechain of Asn13 and that of Tyr14 stick out in opposite directions with respect to the backbone ribbon, since Asn13 and Tyr14 are two consecutive residues of a β-sheet. Thus the relative position of the Tyr14–Tyr15 segment to the Gly5–Ala7 segment is defined. In summary, the Phe12–Asn13 segment of the 'tail' is above the Gly1–Trp3 segment of the 'ring', and the Tyr14–Tyr15 segment of the 'tail' is below the Gly5–Ala7 segment of the 'ring' in the view of Figure 5. Thus the 'lasso' structure is deduced directly on the basis of the critical NOEs. This remarkable structural feature is also confirmed by the structure calculation involving all experimental data as shown in Figure 3.

In order to obtain further information to support this folding of RES-701-1, the susceptibility to temperature of the amide proton chemical shifts was investigated. The amide protons of Ala7, Asp9, Phe12 and Tyr14 which are involved in the hydrogen bonds in the β-sheet segment are expected to possess low temperature coefficients. On the contrary, the amide proton of Asn13 is expected to exhibit a large temperature coefficient because the amide proton of Asn13 is not involved in the hydrogen bonds of the β-sheet segment. The results are shown in Figure 2. Although the susceptibility to temperature of the amide proton chemical shifts of Ala7, Asp9 and Tyr14 were low as expected (ca < 1 ppb K^{-1}), those of Asn13 were also low (ca < 1 ppb K^{-1}), contrary to the expectation. These residues also exhibit very slow amide proton H–D exchange rates (Fig. 2); amide protons of these residues were observed even after 17 h from the addition of D_2O. The unexpectedly low susceptibility to temperature of the amide proton chemical shifts of Asn13 can be explained by the obtained structure. In Figure 5, the amide proton of Asn13 can be considered to be hydrogen bonded to the carbonyl oxygen of Asn2, since the distance between these atoms is only 2.0 Å. Thus the results of the susceptibility to temperature of the amide proton chemical shifts are rationally explained by the obtained structure.

From these results, we concluded that RES-701-1 adopts the 'lasso' structure. From NMR analysis of the synthetic RES-701-1 we found that the 3-D structure of the synthetic RES-701-1 is completely different from that of the authentic RES-701-1.[28] No NOEs were observed between the 'tail' and the 'ring' in the synthetic RES-701-1, suggesting that it does not adopt the 'lasso' structure observed in the authentic RES-701-1. Although both peptides were confirmed to possess the same primary structures by NMR and FABMS, the synthetic RES-701-1 does not exhibit the activity.[27,28] Therefore we suggest here that it is the 'lasso' structure of the authentic RES-701-1 that possesses the ET_B selective activity and not the structure of the synthetic RES-701-1. The details of the comparison between the synthetic and the authentic RES-701-1 will be reported elsewhere.[28]

Recently, a folding similar to RES-701-1, was reported by Frèchet *et al.* for anti-HIV protein RP 71955.[24] RP 71955 consists of 21 amino acid residues with 2 disulfide bonds and the same internal linkage as that of RES-701-1, i.e., the internal linkage between β-carbonyl group of Asp9 and α-amino group of the N-terminal residue (Fig. 1). The Cys7–Asp9 segment in the 'ring' region of RP 71955 was involved in the β-sheet structure, and this position of the β-sheet segment is the same as that of RES-701-1. Since the rmsd of the 'ring' region between the average structure of RES-701-1 and that of RP 71955 was only 1.0 Å, the internal linkage may play a role in determining the structure of the 'ring' region.

In the 3-D structure of RP 71955 determined by Fréchet *et al.*, the 'tail' (Phe10–Trp21) passes through the 'ring' region (Cys1–Asp9) and this way of folding is the same as that of RES-701-1. Recently, on the basis of a survey

of Brookhaven Protein Data Bank, the knot-in-protein structure was independently investigated by two research groups.[29,30] In all the examples, metal atoms tightly bound to the sidechains are included in the formation of the knot structure.[29] Thus it is suggested that the structures of RES-701-1 and RP 71955 are the first examples of a knot structure without metal atoms. RES-701-1 was found to exhibit resistance to protease digestion[19] and RP 71955 was also reported to possess resistance to protease V8 digestion,[24] even though both peptides are very small. Therefore the observed extraordinary folding could be responsible for their remarkable resistance to protease digestion.

It is impossible to make the 'tail' pass through the preformed 'ring' because of steric hindrance. Therefore, the only way to make such a structure is to close the ring after appropriate folding. A similar enzyme may be responsible for this particular closure after adequate folding of the peptide, Since RES-701-1 and RP 71955 were obtained from the same bacteria, *Streptamyces*.

Hypotheses for the structure–activity relationship

Figure 1 shows the amino acid sequence of ETs and ET-antagonists. There are two homologous sites between ETs and RES-701-1. One is the C-terminal residue Trp, and the other is the two consecutive aromatic residues in both RES-701-1 (Trp10–Phe11 or Phe11–Phe12, or Tyr14–Tyr15) and ETs (Tyr13–Tyr14/Phe14). On the basis of the solution structure of ET-3, Mills *et al.* reported that the hydrophobic core was composed of Tyr14, Leu17, Ile19, Ile20 and Trp21, and that the removal of the Trp21 residue disrupted this core.[10] It indicated that Trp21 in ETs is indispensable for keeping the C-terminal conformation. On the other hand, since the C-terminal deletion analog of RES-701-1 exhibits activity similar to that of the native one,[31] the C-terminal Trp of RES-701-1 is not responsible for its activity. Thus the role of the C-terminal Trp of RES-701-1 is expected to differ from that of ETs. Therefore we will not consider structure–activity relationships on the C-terminal Trp hereafter.

As for the other homologous region, replacement of Phe14 to Ala in ET-1 results in a complete loss of activity.[32] Thus aromaticity in position 14 is necessary. The solution structure of ET-3 reported by Mills *et al.* indicated that the hydrophobic core which is important for the activity is composed of two aromatic rings and several methyl groups.[10] In RES-701-1, eight aromatic residues and two methyl groups are included in the whole 16 amino acid residues. Among them, five aromatic residues (Trp10, Phe11, Phe12, Tyr14 and Tyr15) are in the 'tail' region, and two methyl groups (Thr6 and Ala7) are in the 'ring' region. Also as indicated before, two consecutive aromatic residues of RES-701-1 in the 'tail' region are also present in ET-3. Looking at the structure in Figure 5, only Tyr14–Tyr15 are spatially close to the methyl groups of Thr6 and Ala7 among the two consecutive aromatic residues listed above. Therefore the region containing Thr6, Ala7, Tyr14 and Tyr15 may mimic the hydrophobic core of ET-3.

Another hypothesis can be considered. Recently the most potent nonselective antagonist to date, SB209670 was obtained by Eliott *et al.*[25] They suggested that two aromatic rings and one carboxylic acid of SB209670 (aromatic rings labeled 1 and 2, and carboxylic acid labeled 3 in Figure 1) mimic two consecutive aromatic residues, Tyr13 and Phe14, and one acidic residue, Asp18 of ET-1, respectively. In RES-701-1, no acidic residue was present, but there are three segments of two consecutive aromatic residues. When the two consecutive aromatic rings of Tyr14–Tyr15 of RES-701-1 are fitted to two aromatic rings of SB209670, the position of Asn2 of RES-701-1 corresponds to the carboxylic acid of SB209670. When the other two consecutive aromatic residues of RES-701-1 are fitted, nothing is found at the position of the carboxylic acid of SB209670. Figure 5 shows that Tyr14–Tyr15 and Asn2 are spatially close. Since Asn2 has a carbonyl oxygen in the side chain, this atom may play the role of a proton-acceptor instead of the Asp of ETs. Therefore, the two consecutive aromatic residues Tyr14–Tyr15 and the Asn2 of RES-701-1 may mimic Tyr13–Phe14/Tyr14 and Asp18 of ETs, respectively.

It is often observed that the β-turn is a structural motif in many biologically active cyclic peptides and it has been postulated in many cases to be the biologically active form of linear peptides.[33] The regions of the residues 9–12 and the residues 4–7 in RES-701-1, and that of the residues 5–8 in ETs adopt a β-turn. However, it has been shown that the linear peptide, IRL-1620 [suc-$E^{9}A^{11,15}$ET-1(8–21)], which does not include the turn region of ET, exhibits potent ET_B selective agonist activity.[34] Therefore ET_B selective binding activity is not brought about by the N-terminal region in which the turn is included, but by the 8–21 region of ET. Thus the β-turn region may not be required for the binding activity.

In conclusion, our study has shown that the ET_B selective antagonist RES-701-1 in DMSO solution adopts a highly ordered and extraordinary structure. The obtained structure suggests that the region consisting of Thr6, Ala7, Tyr14 and Tyr15 and/or the region consisting of Asn2, Tyr14 and Tyr15 are involved in binding with receptor. The general structural motif of RES-701-1 in DMSO, i.e., the 'lasso' structure is not an artifact of the solvent used because the 'tail' cannot 'pass through' or 'pass back out' once the 'ring' has been formed. In addition, NMR analysis of RES-701-1 in 60% ethylene glycol:40% water mixture solution revealed that RES-701-1 takes almost the same conformation as determined in DMSO solution (data not shown). The DMSO solution structure must therefore be a close representation of the bio-active conformation. Experiments are now on going to investigate the structure–activity relationship using the derivatives of RES-701-1.

Experimental

NMR experiment

Since RES-701-1 could not be dissolved in H_2O, NMR experiments were carried out in deuterated dimethyl sulphoxide (DMSO-d_6) at a concentration of 3 mM. NMR spectra were recorded at 30 °C on BRUKER AM-500 and JEOL JNM-A400 spectrometers. Chemical shifts were referenced to the methyl proton resonance of DMSO at 2.5 ppm.

Two dimensional nuclear Overhauser effect spectroscopy (NOESY),[35] double quantum filtered shift correlated spectroscopy (DQF-COSY)[36] and homonuclear Hartmann–Harn spectroscopy (HOHAHA)[37] spectra in a phase sensitive mode using time proportional phase incrementation, and exclusive COSY (E.COSY)[38] spectra in States mode, were recorded, respectively. Spectra were mostly collected with 512 complex points in t_1 and 2048 complex points in the t_2 dimension. The t_2 FIDs were multiplied by a shifted sine-bell square window function and then Fourier transformed. The t_1 data were apodized with the same window function, zero-filled to 2048 complex points, and then Fourier transformed. The NOESY spectra were collected with two mixing times, 100 ms and 300 ms. The NOESY spectrum with the longer mixing time was used for the signal assignments and that with the shorter one was used to obtain the distance information. The $^3J_{NH\alpha}$ coupling constants were obtained from the high resolution 1-D spectra (0.48 Hz point^{-1}) multiplied by the Gaussian window function, except the residues Gly1, Gly5, Thr6 and Phe12, for which the coupling constants were not obtained, due to the degeneracies of amide protons. The $^3J_{\alpha\beta}$ coupling constants for the residues Asn2, His4, Asp9, Trp10, Phe11, Phe12, Asn13 and Trp16 were measured from the E.COSY spectrum with a high resolution in the F2 dimension (0.85Hz point^{-1}). Owing to the degeneracies of β-protons, this coupling constant could not be obtained for the residues Trp3, Tyr14 and Tyr15.

Aggregation in peptides gave rise to concentration-dependent line widths.[39,40] Dilution by a factor of 100, of the sample concentration used, did not significantly change the chemical shifts or line widths, which showed the absence of aggregate species.

Calculation

In order to make the ring conformation of RES-701-1, the chemical structure of Asp9 was modified by the MolEdit program in MolSkop system (JEOL Co. Ltd,) on a TITAN computer.

The distance constraints were obtained by the volume integration of NOESY cross peaks obtained at 30 °C, using the NMR2 software (NMRi Inc.) on a TITAN computer. The 142 ^1H–^1H distance constraints (62 intraresidue, 37 sequential, 13 medium-range ($1 < i-j \leq 3$) and 30 long-range ($i-j > 3$) NOES, 11 ϕ angles and 8 $\chi 1$ angles were used for calculations. The distance constraints for the hydrogen bonds were not used in the calculations.

The solution structures of RES-701-1 were obtained by the combined use of DG and SA calculations. DG calculations were carried out by the DADAS90 program in MolSkop system on a TITAN computer. Starting from initial structures with randomly chosen dihedral angles, the structures with the best satisfied distance and angle constraints were obtained. SA calculations for refinement and NOESY back calculations were carried out by the X-PLOR[39] program on an IRIS Indigo R4000 computer. The time step of dynamics was set to 5 fs during the SA calculations. Force constants for the NOE constraints and dihedral angle constraints were maintained at 50 kcal mol^{-1} Å^{-2} and 200 kcal mol^{-1} rad^{-2}, respectively, throughout the refinement process. The system was cooled stepwise from 1000K to 100K in 50K decrements via 10 ps restraint dynamics during which the repulsive term was increased linearly from 0.003 to 4 kcal mol^{-1} Å^{-4}. Final structures were obtained after 1000 cycles of Powell minimization. Finally, 46 well-converged structures were obtained.

NOESY back calculations

NOESY back calculations were carried out using a full-relaxation matrix. The R-factor was used to evaluate the differences between the experimental and calculated NOE intensities; $R = (I_o - I_c)/I_o$, where I_o = experimental and I_c = calculated intensity, respectively.

The 3-D structure of RP 71955 was obtained from the Brookhaven Protein Data Bank.

Acknowledgment

The authors thank Dr Fujita (JEOL Co. Ltd) for his support in constructing the molecule in MolSkop. R. K. greatly acknowledges Dr M. Kono, Dr M. J. Dooley and Dr N. Kagami for their careful reading of this manuscript, Dr Y. Oda and Dr M. Katahira (Yokohama National University) for their helpful discussions on this manuscript and Dr H. Nakamura (Protein Research Institute) for his stimulating discussion on this manuscript.

References

1. Yanagisawa, M.; Kurihara, H.; Kimura, S.; Tomobe, Y.; Kobayashi, M.; Mitui, Y.; Yazaki, Y.; Goto, K.; Masaki, T. *Nature* **1988**, *332*, 411.

2. Inoue, A.; Yanagisawa, M.; Kimura, S.; Kasuya, Y.; Miyauchi, T.; Goto, K.; Masaki, T. *Proc. Natl Acad. Sci. U.S.A.* **1989**, *86*, 2863.

3. Arai, H.; Hori, S.; Aramori, I.; Ohkubo, H.; Nakanishi, S. *Nature* **1990**, *348*, 730.

4. Lin, H. Y.; Kaji, E. H.; Winkel, G. K.; Ives, H. E.; Lodish, H. F. *Proc. Natl Acad. Sci. U.S.A.* **1991**, *88*, 3185.

5. Hosoda, K.; Nakao, K.; Arai, H.; Suga, S.-L.; Ogawa, Y.; Mukoyama, M.; Shirakama, G.; Saito, Y.; Nakanishi, S.; Imura, H. *FEBS Lett.* **1991**, *287*, 23.

6. Sakurai, T.; Yanagisawa, M.; Takuwa, Y.; Miyazaki, H.; Kimura, S.; Goto, K.; Masaki, T. *Nature* **1990**, *348*, 732.

7. Nakamura, M.; Takayanagi, R.; Sakai, Y.; Sakamoto, S.; Hagiwara, H.; Mizuno, T.; Saito, Y.; Hirose, S.; Yamamoto, M.; Nawata, H. *Biochem. Biophys. Res. Commun.* **1991**, *177*, 34.

8. Ogawa, Y.; Nakao, K.; Arai, H.; Nakanishi, S.; Imura, H. *Biochem. Biophys. Res. Commun.* **1991**, *178*, 248.

9. Doherty, M. *J. Med. Chem.* **1992**, *35*, 1493.

10. Mills, R. G.; O'Donoghue, S. I.; Smith R.; King, G. F. *Biochemistry* **1992**, *31*, 5640.

11. Aumelas, A.; Chiche, L.; Mahe, E.; Le-Nguyen, D.; Sizun, P.; Berhault, P.; Perly, D. *Neurochem. Int.* **1991**, *18*, 471.

12. Bortmann, P.; Hoflack, J.; Pelton, J. T.; Saudek, V. *Neurochem. Int.* **1991**, *18*, 491.

13. Endo, S.; Inooka, H.; Ishibashi, Y.; Kitada, C.; Mizuta, E.; Fujino, M. *FEBS Lett.* **1989**, *257*, 149.

14. Krystek, S. R.; Bassolino, D. A.; Novotny, J.; Chen, C.; Marchener, T. M.; Anderson, N. H. *FEBS Lett.* **1991**, *281*, 212.

15. Mills, R. G.; Atkins, A. R.; Harvey, T.; Jinius, F. K.; Smith, R.; King, G. F. *FEBS Lett.* **1991**, *282*, 247.

16. Saudek, V.; Hoflack, J.; Pelton, J. T. *Int. J. Pept. Protein Res.* **1991**, *37*, 174.

17. Saudek, V.; Hoflack, J.; Pelton J. T. *FEBS Lett.* **1989**, *257*, 145.

18. Morishita, Y.; Chiba, S.; Tsukuda, E.; Tanaka, T.; Ogawa, T.; Yamasaki, M.; Yoshida, M.; Kawamoto, I.; Matsuda, Y. *J. Antibiotics* **1994**, *47*, 269.

19. Yamasaki, M.; Yano, K.; Yoshida, M.; Matsuda, Y.; Yamaguchi, K. *J. Antibiotics* **1994**, *47*, 276.

20. Atkinson, R. A.; Pelton, J. T. *FEBS Lett.* **1992**, *296*, 1.

21. Reily, M. D.; Venkataraman, T.; Omecinsky, D. O.; Dunbar, Jr J. B.; Doherty, A. M.; DePue, P. L. *FEBS Lett.* **1992**, *300*, 136.

22. Krystek, Jr S. R.; Bassolino, D. A.; Bruccoleri, R. E.; Hunt, J. T.; Porubcan, M. A.; Wandler, C. F.; Andersen, N. H. *FEBS Lett.* **1992**, *299*, 255.

23. Coles, M.; Sowemmimo, V.; Scanlon, D.; Munro, S. L. A.; Craik, D. J. *J. Med. Chem.* **1993**, *36*, 2658.

24. Frèchet, D.; Guitton, L. D.; Herman, D.; Faucher, G.; Helynck, B.; du Sorbier, M.; Ridoux, J. P.; James-Surcouf, E.; Vuilhorgne, M. *Biochemistry* **1994**, *33*, 42.

25. Eliott, J. D.; Lago, M. A.; Cousins, R. D.; Gao, A.; Leber, J. D.; Erhard, K. F.; Nambi, P.; Elchourbagy, N. A.; Kumar, C.; Lee, J. A.; Bean, L. W.; Debrosse, C. W.; Eggleston, D. S.; Brooks, D. P.; Feuestein, G.; Ruffolo, Jr R. R.; Weinstock, J.; Gleason, J. G.; Peishoff, C. E.; Ohlstein, E. H. *J. Med. Chem.* **1994**, *37*, 1553.

26. Wüthrich, K. *NMR of Proteins and Nucleic Acids;* J. Wiley, New York, 1986.

27. He, J. X.; Cody, W. L.; Flynn, M. A.; Welch, K. M.; Reynolds, E. E.; Doherty, A. M. *Bioorg. Med. Chem. Lett.* **1995**, *5*, 621.

28. Katahira, R.; Shibata, K.; Yamasaki, M.; Matsuda, Y.; Yoshida, M. unpublished data.

29. Liang C.; Mislow K. *J. Am. Chem. Soc.* **1994**, *116*, 11189.

30. Mansfield, M. L. *Nat. Struct. Biol.* **1994**, *1*, 213.

31. Yamasaki, M.; Yano, K.; Yoshida, M.; Matsuda, Y.; Yamaguchi, K. personal communication.

32. Nakajima, K.; Kubo, S.; Kumagaye, S.; Nishio, H.; Tsunemi, M.; Inui, T.; Kuroda, H.; Chino, N.; Watanabe, T.; Kimura, T.; Sakakibara, S. *Biochem. Bhiophys. Res. Commun.* **1989**, *163*, 424.

33. Rose, G. D.; Gierasch, L. M.; Smith J. A. *Adv. Protein Chem.* **1985**, *37*, 1.

34. Takai, M.; Umemura, I.; Yamasaki, K.; Watanabe, T.; Fujitani, Y.; Oda, K.; Urade, Y.; Inui, T.; Yamamura, T.; and Okada, T. *Biochem. Biophys. Res. Commun.* **1992**, *184*, 953.

35. Jeener, J.; Meier, B. H.; Bachmann, P.; Ernst, R. R. *J. Chem. Phys.* **1979**, *71*, 4546.

36. Rance, M.; Sorensen, O. W.; Bosenhausen, G.; Wagner, G.; Ernst, R. R.; Wuthrich, K. *Biochem. Biophys. Res. Commun.* **1983**, *117*, 479.

37. Branshweiler, L.; Ernst R. R. *J. Magn. Reson.* **1983**, *53*, 521.

38. Griesinger, C.; Sorensen, O. W.; Ernst, R. R. *J. Am. Chem. Soc.* **1985**, *107*, 6394.

39. Ciela, J. D.; Gilbert, D. E.; Feigon, J. *J. Am. Chem. Soc.* **1991**, *113*, 3957.

40. Osterhout, J. J.; Handel, T.; Na, G.; Toumadje, A.; Long, R. C.; Connolly, P. J.; Hoch, J. C.; Johnson, W. C.; Live, D.; De Grado, W. F. *J. Am. Chem. Soc.* **1992**, *114*, 331.

41. Brünger, A. T. *X-PLOR Version 3.1, User Manual*; Yale University: New Haven, CT, 1990.

(*Received in Japan* 20 *April* 1995; *accepted* 1 *June* 1995)